Electronic Supplementary Information (ESI)

One-pot reductive etherification of biomass-derived 5-hydroxymethylfurfural to 2,5-bis(isopropoxymethyl)furan over a sulfonic acid-functionalized zirconium-based coordination catalyst

Aiyong He,[‡a] Qinyin Gu,[‡a] Xinming Shen,[a] Jingyi Zheng,[a] Lei Hu,[*a] Xiaoyu Wang,[a] Yetao Jiang,[a] Zhen Wu,[*a] Jiaxing Xu[a] and Jinliang Song[*b]

[a] Jiangsu Key Laboratory for Biomass-Based Energy and Enzyme Technology, Jiangsu Collaborative Innovation Center of Regional Modern Agriculture & Environmental Protection, School of Chemistry and Chemical Engineering, Huaiyin Normal University, Huaian 223300, China

[b] School of Chemical Engineering and Light Industry, Guangdong University of Technology, Guangzhou 510006, China

[*] Corresponding Author: hulei@hytc.edu.cn; wuzhen@hytc.edu.cn; songjl_2021@gdut.edu.cn

[‡] These authors contributed equally to this work.

Experimental reagents

5-Hydroxymethylfurfural (HMF, 98%), 2,5-bis(hydroxymethyl)furan (BHMF, 98%), 5-methylfurfural (MF) and 5-methylfurfuryl alcohol (MFA, 98%) were purchased from Saen Chemical Technology Co., Ltd. (Shanghai, China). CT269DR, a macroporous sulfonated resin, was provided by Purolite Co., Ltd. (Huzhou, China). Zirconium oxide (ZrO_2, 99%), zirconium tetrachloride ($ZrCl_4$, 99%) and stannic chloride pentahydrate ($SnCl_4$, 99%) were obtained from Shanghai Aladdin Reagent Co., Ltd. (Shanghai, China). 1,4-Benzenedicarboxylic acid (BDC, 99%) and 2-sulfo-1,4-benzenedicarboxylic acid monosodium (BDC-SO_3Na, 99%) were supplied by Shanghai Jiuding Chemical Co., Ltd. (Shanghai, China). Methanol (MeOH), ethanol (EtOH), n-propanol (nPrOH), isopropanol (iPrOH), n-butanol (nBuOH), sec-butanol (sBuOH), acetic acid (AA), dimethyl formamide (DMF) and other chemicals were purchased from Sinopharm Chemical Reagent Co., Ltd. (Shanghai, China) and used without any purification.

Catalyst characterization

Fourier transform infrared (FT-IR) spectra were recorded on a Nicolet 380 spectrometer. X-ray diffraction (XRD) patterns were performed on a Bruker D8 Advance diffractometer with a Cu Kα radiation source (λ=0.15418 nm). Scanning electron microscopy (SEM), high-resolution transmission electron microscopy (HR-TEM) and high-angle annular dark-field scanning transmission electron microscopy (HAADF-STEM) images were carried out on a Zeiss Supra55 microscope, a JEM-2100f microscope and a FEI Titan Themis G2 F30 microscope, respectively. Element contents

were determined by a VISTA-MPX inductively coupled plasma atomic emission spectrometer (ICP-AES) and a Vario EL III elemental analyzer (EA), respectively. Nitrogen adsorption-desorption (NAD) isotherms were measured on a ASAP 2020 physisorption analyzer at 77 K. Temperature-programmed desorption (TPD) profiles, X-ray photoelectron spectroscopy (XPS) spectra and pyridine-adsorbed FT-IR spectra were collected on an AutoChem II 2920 chemisorption analyzer, an Escalab 250Xi spectrometer with an Al Kα excitation source ($h\nu$ = 1486.6 eV) and a Bruker Tensor 27 spectrometer in the range of 1300 to 1700 cm^{-1}, respectively.

2,5-Bis(isopropoxymethyl)furan (BIPMF) synthesis

In order to synthesize the standard BIPMF (Scheme S1), 1 g BHMF, 0.25 g CT269DR and 49 g iPrOH were added into a stainless steel autoclave with a mechanical stirrer, which was sealed and heated to 50 °C under a stirring rate of 400 rpm. After 24 h, the autoclave was cooled to room temperature (RT). Note that BHMF conversion and BIPMF selectivity were greater than 99% (Fig. S1). Next, CT269DR was removed from the reaction mixture by filtration, and then, the filtrate was distilled at 60 °C for 1 h under the reduced pressure to remove the low-boiling iPrOH and H_2O. Subsequently, the remnant was renewedly dissolved in 25 mL ethyl acetate (EtOAc), which was followed by adding 0.25 g activated carbon (AC). After 10 min under vigorous agitation, the mixture was further filtered and distilled to obtain the pure BIPMF. Finally, the pure BIPMF was confirmed by gas chromatography-mass spectrometry (GC-MS, Agilent 5977B) (Fig. S2) and nuclear magnetic resonance (NMR)

spectrometry (Bruker ADVANCE II) (Fig. S3), which were in accordance with the results of Tang and co-workers.[1]

5-(Isopropoxymethyl)furfural (IPMF) synthesis

In order to synthesize the standard IPMF (Scheme S2), 1 g HMF, 0.25 g CT269DR and 49 g iPrOH were added into a stainless steel autoclave with a mechanical stirrer, which was sealed and heated to 60 °C under a stirring rate of 400 rpm. After 24 h, the autoclave was cooled to RT. Note that HMF conversion and IPMF selectivity were greater than 99% (Fig. S4). Next, other procedures were the same to those of BIPMF. Finally, the pure IPMF was confirmed by GC-MS (Fig. S5) and NMR (Fig. S6), which were in accordance with the results of Wang and co-workers.[2]

5-Methyl-2-isopropoxymethylfuran (MIPMF) synthesis

In order to synthesize the standard MIPMF (Scheme S3), 1 g MFA, 0.25 g CT269DR and 49 g iPrOH were added into a stainless steel autoclave with a mechanical stirrer, which was sealed and heated to 50 °C under a stirring rate of 400 rpm. After 20 h, the autoclave was cooled to RT. Note that MFA conversion and MIPMF selectivity were greater than 99% (Fig. S7). Next, other procedures were the same to those of BIPMF. Finally, the pure MIPMF was confirmed by GC-MS (Fig. S8) and NMR (Fig. S9), which were in accordance with the results of Tang and co-workers.[1]

Product analysis

The liquid samples were analyzed by GC and GC-MS. For analysis, the injector temperature and detector temperature were set to 300 °C. Meanwhile, the initial

column temperature was 40 °C and maintained for 2 min, and then, the column temperature was elevated to 100 °C with a heating rate of 5 °C/min and maintained for 2 min, after that, the column temperature was further elevated to 250 °C with a heating rate of 10 °C/min and maintained for 1 min. Moreover, HMF, BHMF, IPMF, HIPMF, BIPMF and MIPMF were based on the following equations:

$$\text{HMF conversion (\%)} = (1-\frac{\text{Mole of HMF in products}}{\text{Initial mole of HMF}}) \times 100 \quad (1)$$

$$\text{BHMF yield (\%)} = \frac{\text{Mole of BHMF in products}}{\text{Initial mole of HMF}} \times 100 \quad (2)$$

$$\text{IPMF yield (\%)} = \frac{\text{Mole of IPMF in products}}{\text{Initial mole of HMF}} \times 100 \quad (3)$$

$$\text{HIPMF yield (\%)} = \frac{\text{Mole of HIPMF in products}}{\text{Initial mole of HMF}} \times 100 \quad (4)$$

$$\text{BIPMF yield (\%)} = \frac{\text{Mole of BIPMF in products}}{\text{Initial mole of HMF}} \times 100 \quad (5)$$

$$\text{MIPMF yield (\%)} = \frac{\text{Mole of MIPMF in products}}{\text{Initial mole of HMF}} \times 100 \quad (6)$$

Catalyst recovery

To study the recyclability of Zr-BDC-S_{60}, when each reaction run was finished, the catalyst was separated by centrifugation from the reaction mixture, and washed with the ultrapure water (UPW) and EtOH for five times, respectively. After drying at 80 °C for 12 h in a vacuum oven, the recovered catalyst was directly used for the next reaction run under the same reaction conditions.

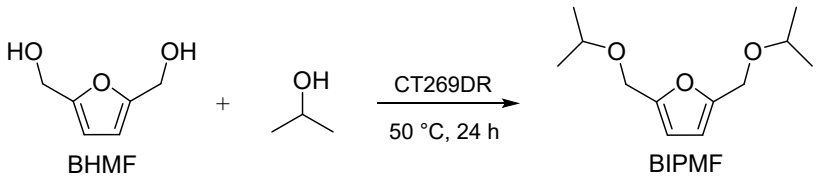

Scheme S1 Synthesis of BIPMF in iPrOH over CT269DR. Reaction conditions: 1 g BHMF, 0.25 g CT269DR, 49 g iPrOH, 50 °C, 24 h.

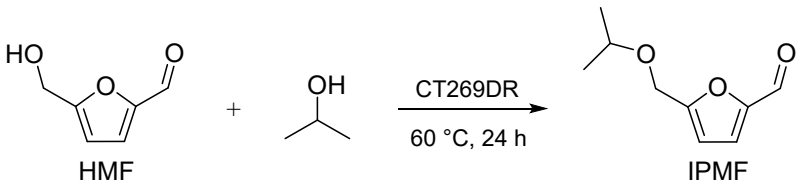

Scheme S2 Synthesis of IPMF in iPrOH over CT269DR. Reaction conditions: 1 g HMF, 0.25 g CT269DR, 49 g iPrOH, 60 °C, 24 h.

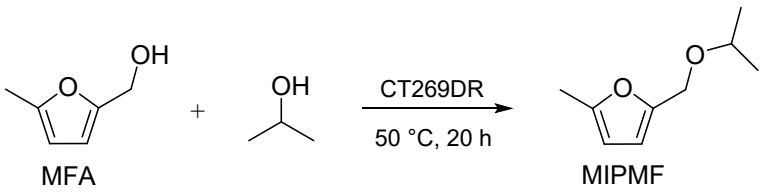

Scheme S3 Synthesis of MIPMF in iPrOH over CT269DR. Reaction conditions: 1 g MFA, 0.25 g CT269DR, 49 g iPrOH, 50 °C, 20 h.

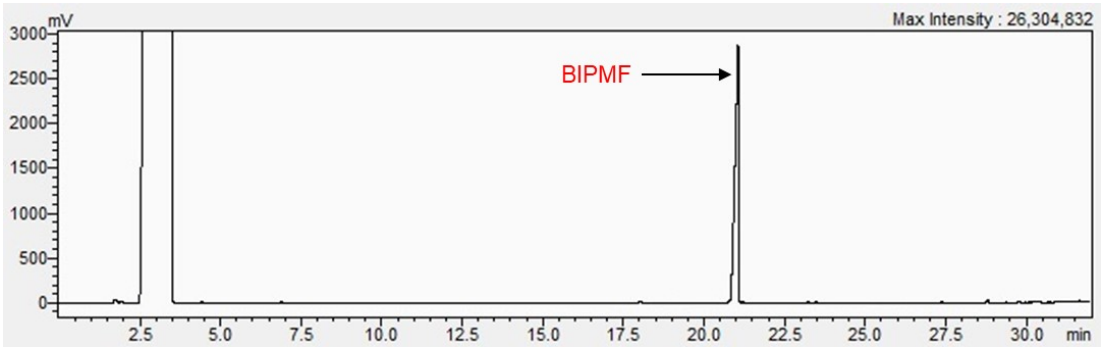

Fig. S1 GC chromatogram for the etherification of BHMF to BIPMF over CT269DR.

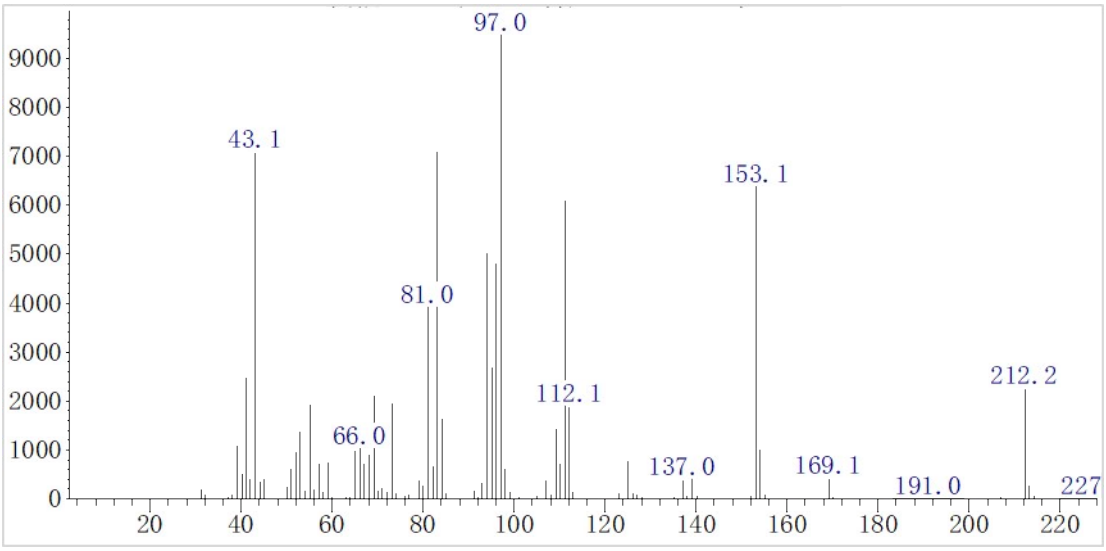

Fig. S2 MS spectrum of BIPMF.

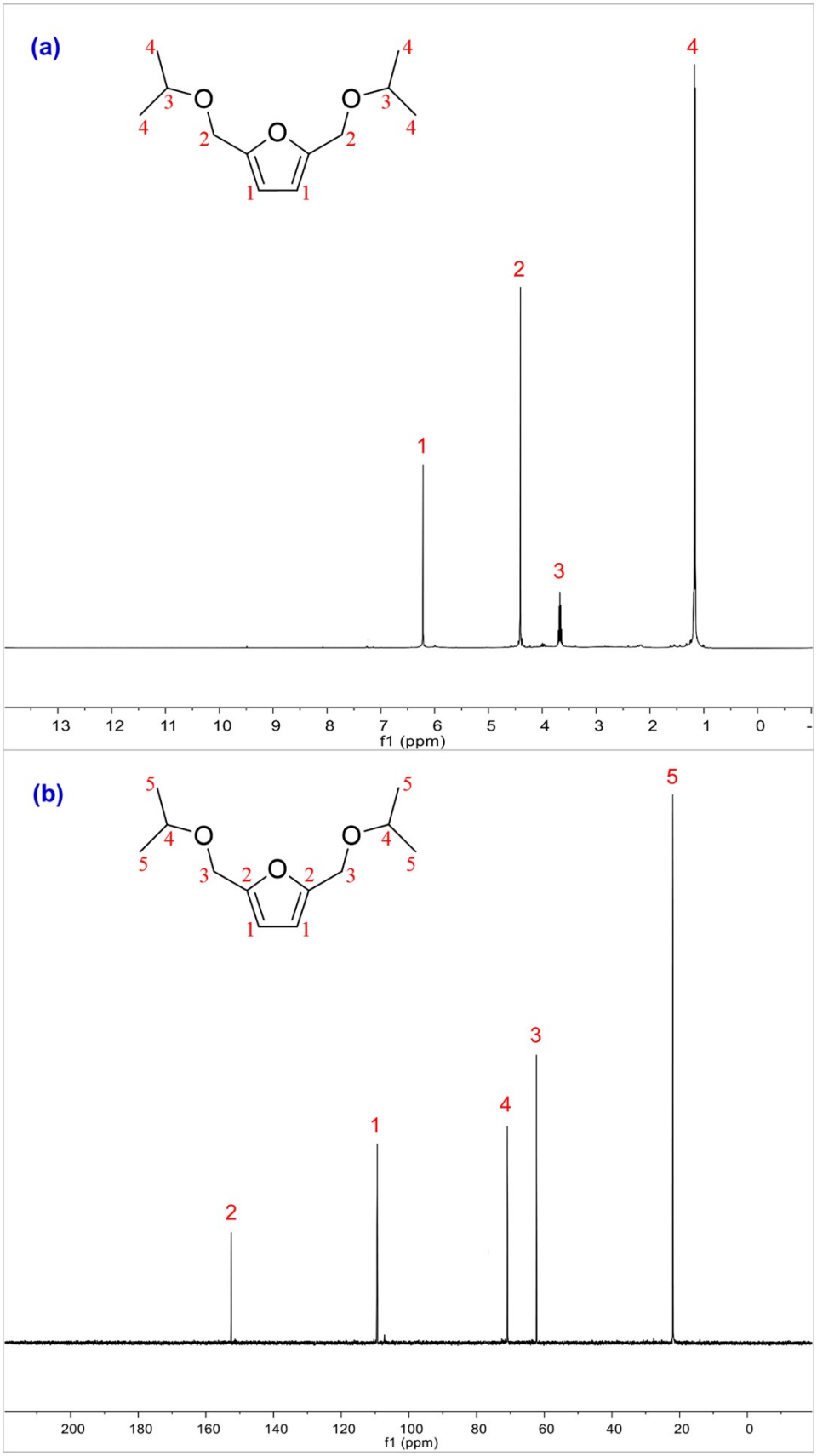

Fig. S3 ^{1}H NMR (a) and ^{13}C NMR (b) of BIPMF in $CDCl_3$.

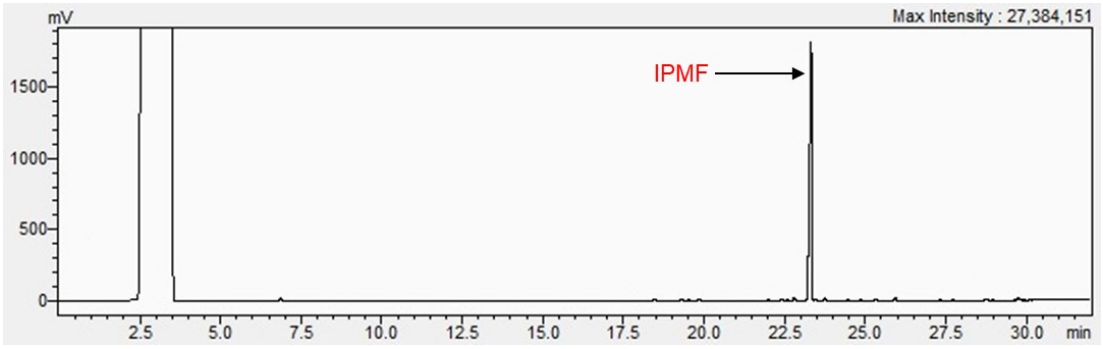

Fig. S4 GC chromatogram for the etherification of HMF to IPMF over CT269DR.

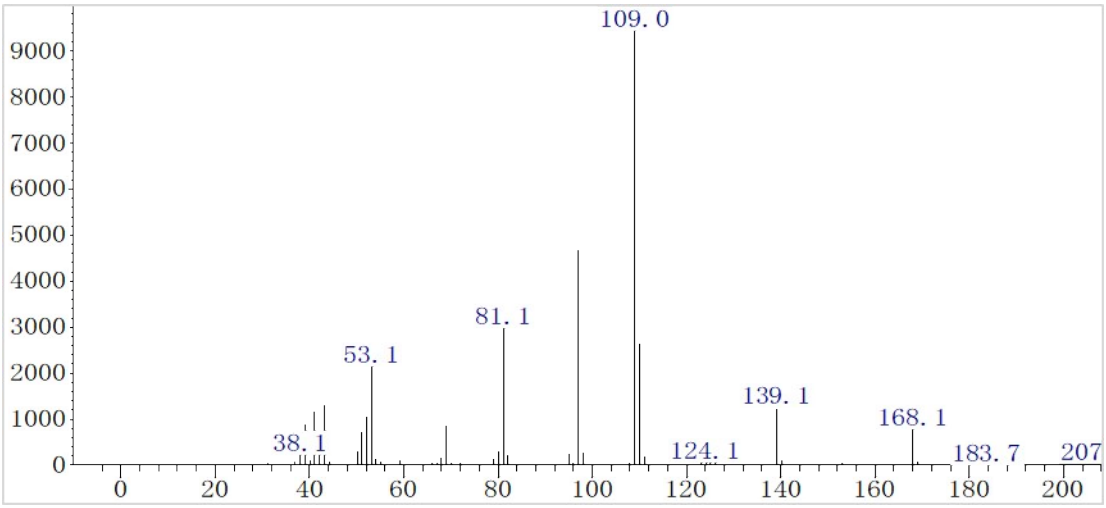

Fig. S5 MS spectrum of IPMF.

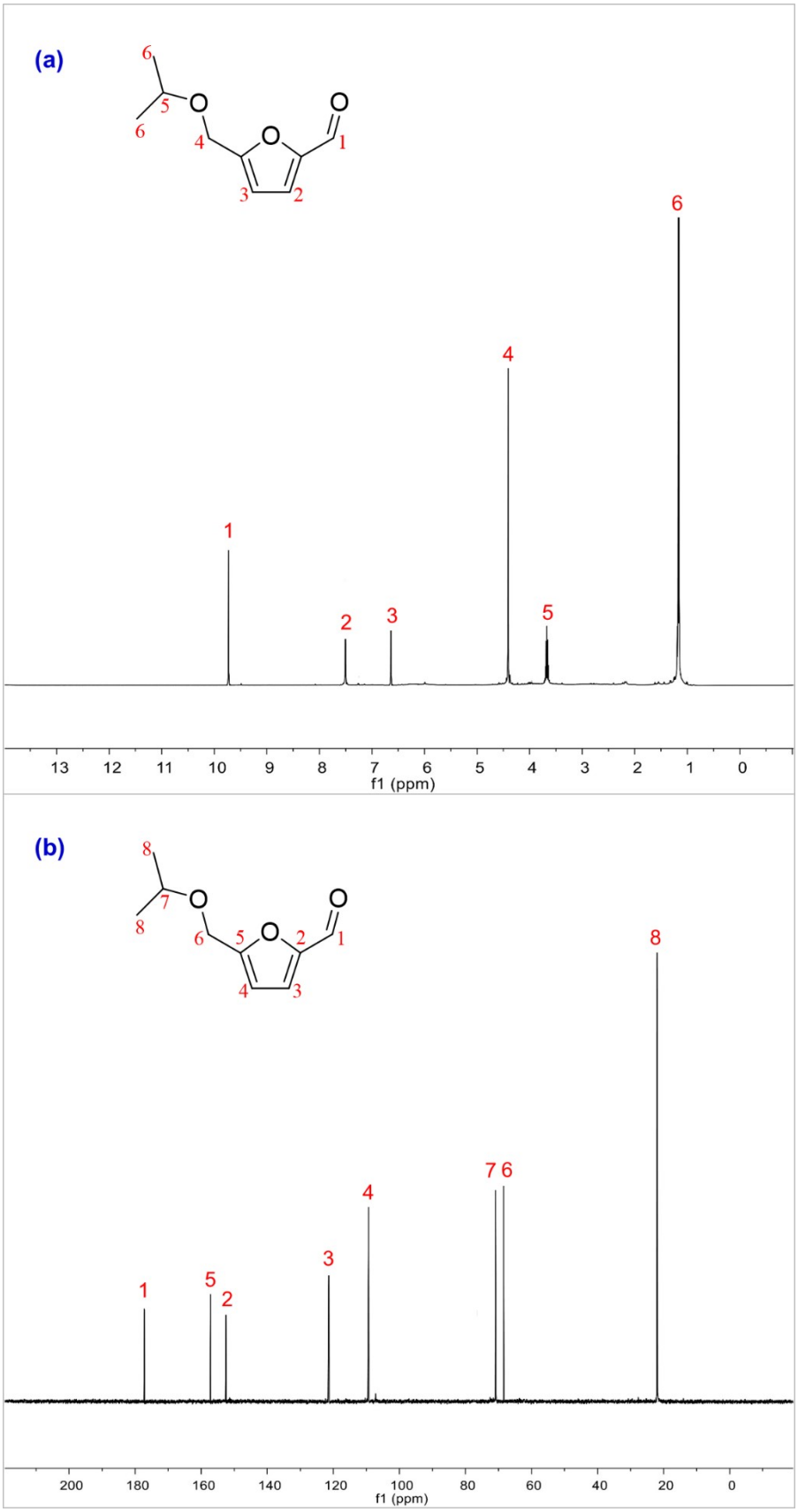

Fig. S6 ^{1}H NMR (a) and ^{13}C NMR (b) of IPMF in $CDCl_3$.

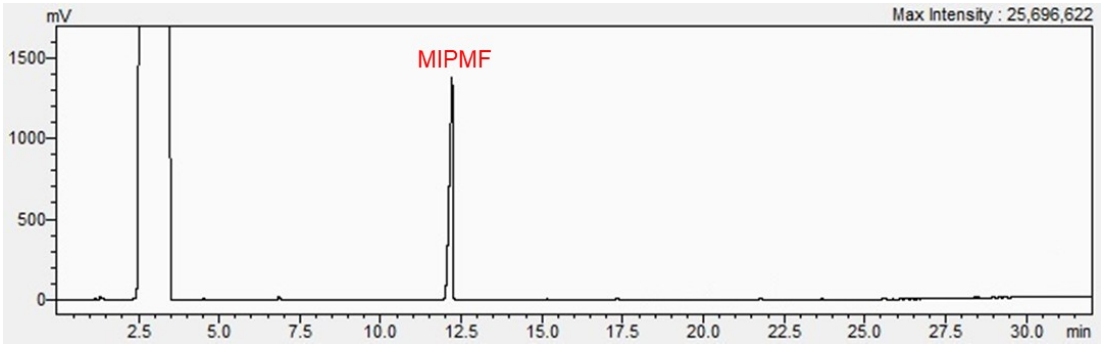

Fig. S7 GC chromatogram for the etherification of MFA to MIPMF over CT269DR.

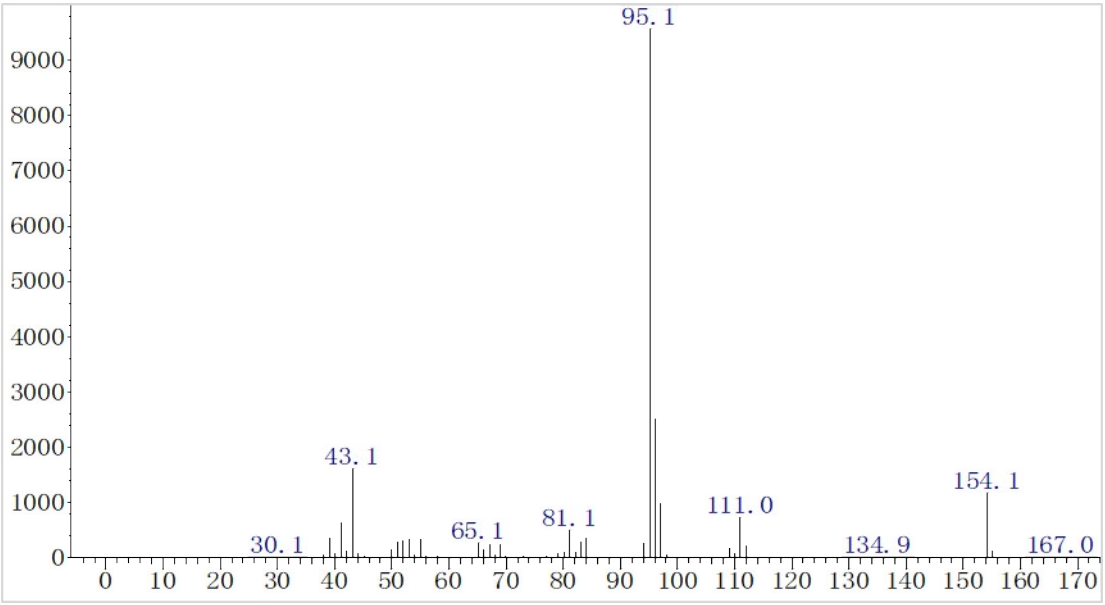

Fig. S8 MS spectrum of MIPMF.

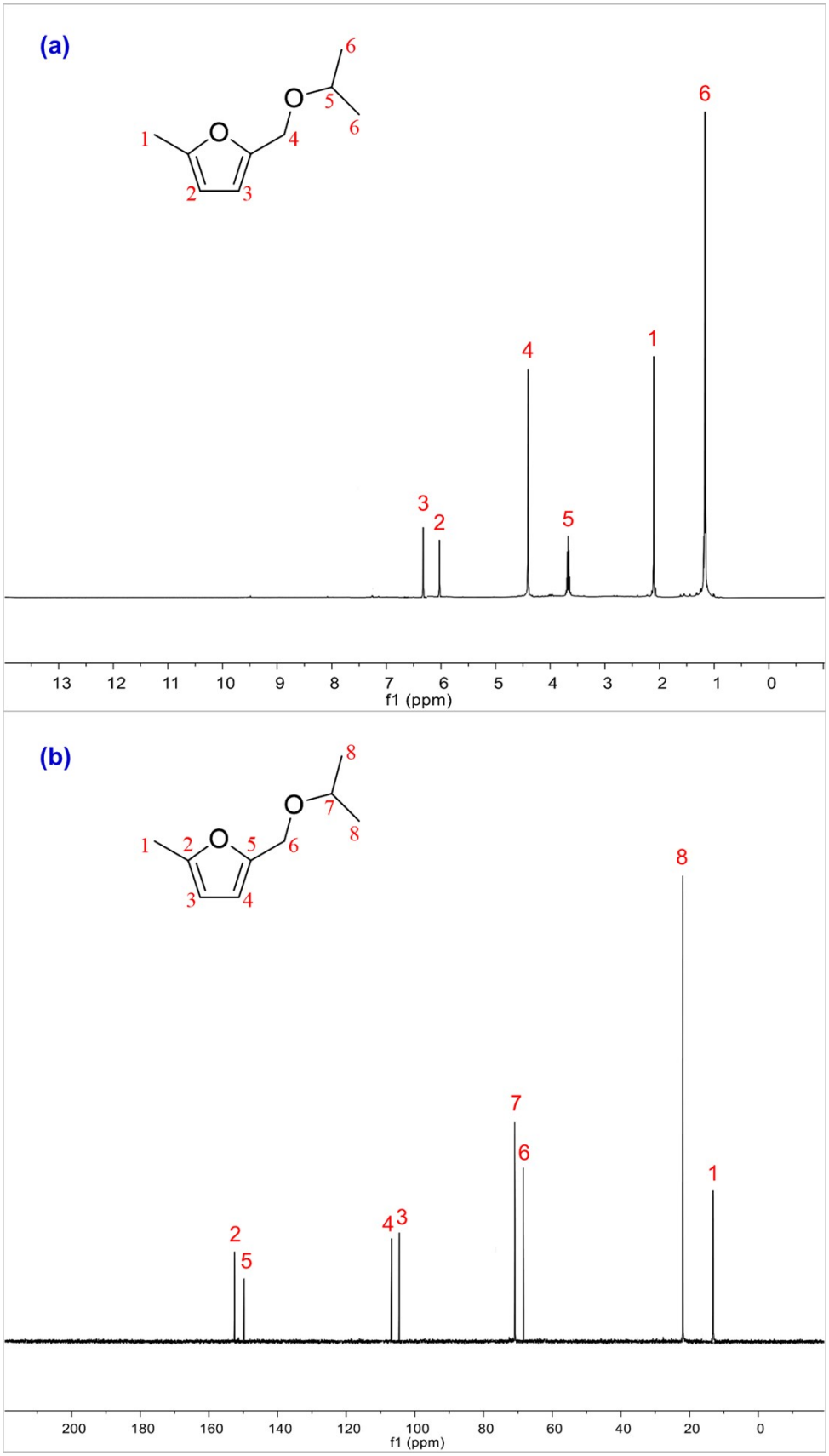

Fig. S9 ^{1}H NMR (a) and ^{13}C NMR (b) of MIPMF in $CDCl_3$.

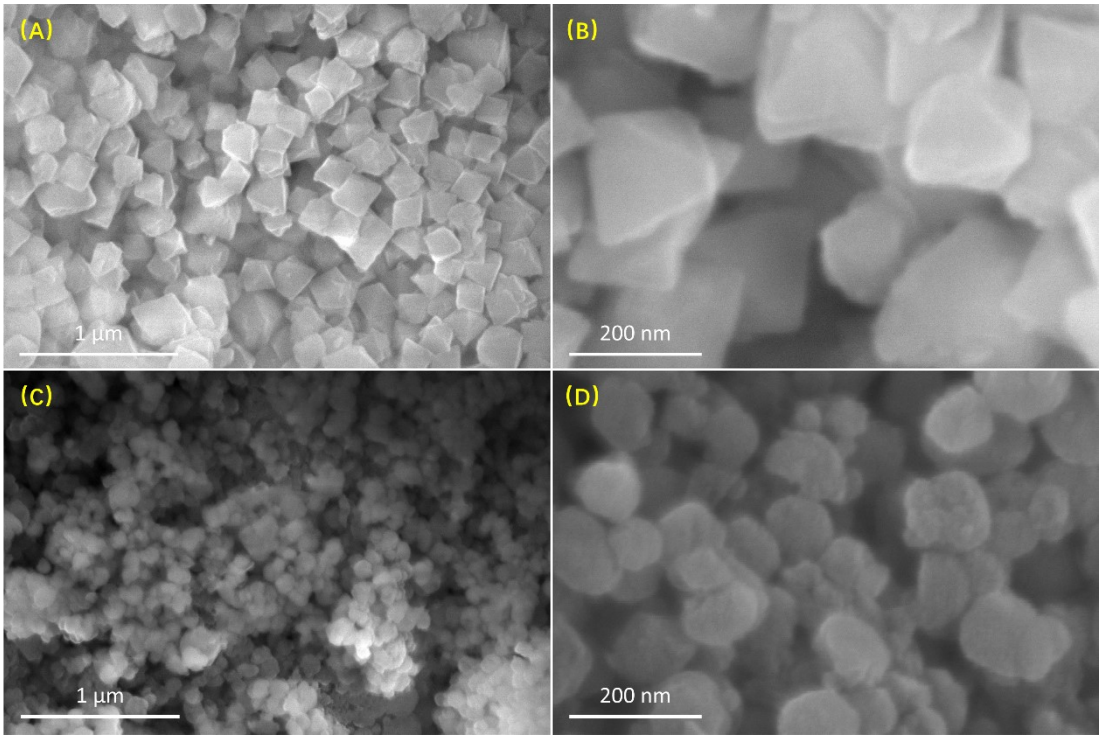

Fig. S10 SEM images of Zr-BDC (A and B) and Zr-BDC-S_{100} (C and D).

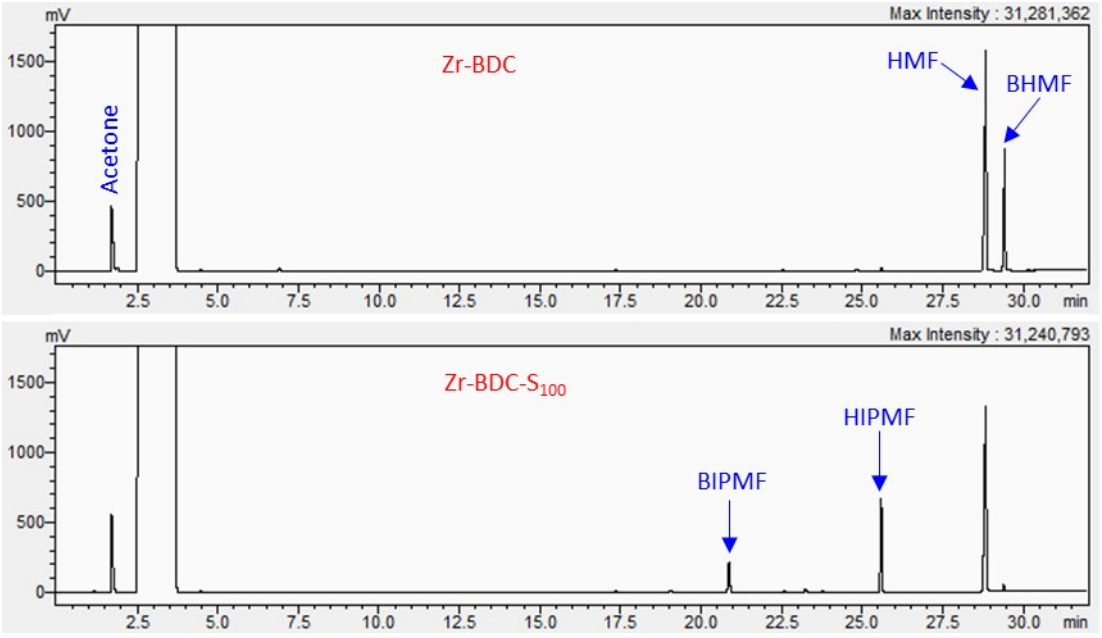

Fig. S11 GC chromatograms for the one-pot reductive etherification of HMF to BIPMF over Zr-BDC and Zr-BDC-S_{100}. Reaction conditions: 0.25 g HMF, 19.75 g iPrOH, 0.1 g catalyst, 120 °C, 2 h.

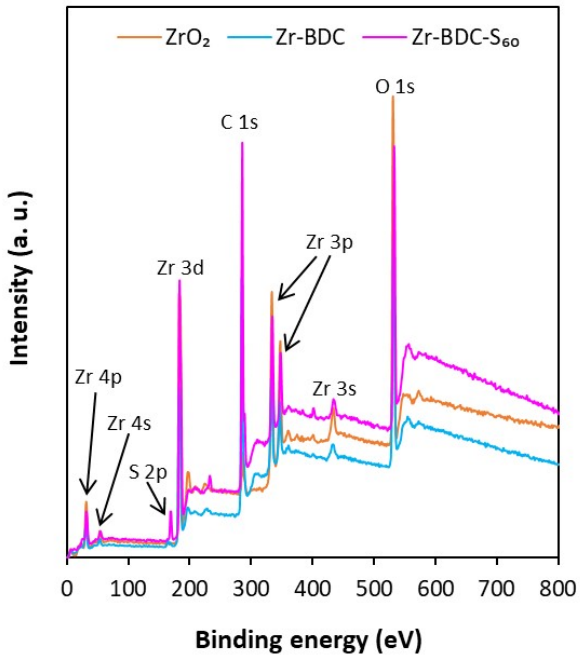

Fig. S12 XPS survey scan spectra of ZrO_2, Zr-BDC and Zr-BDC-S_{60}.

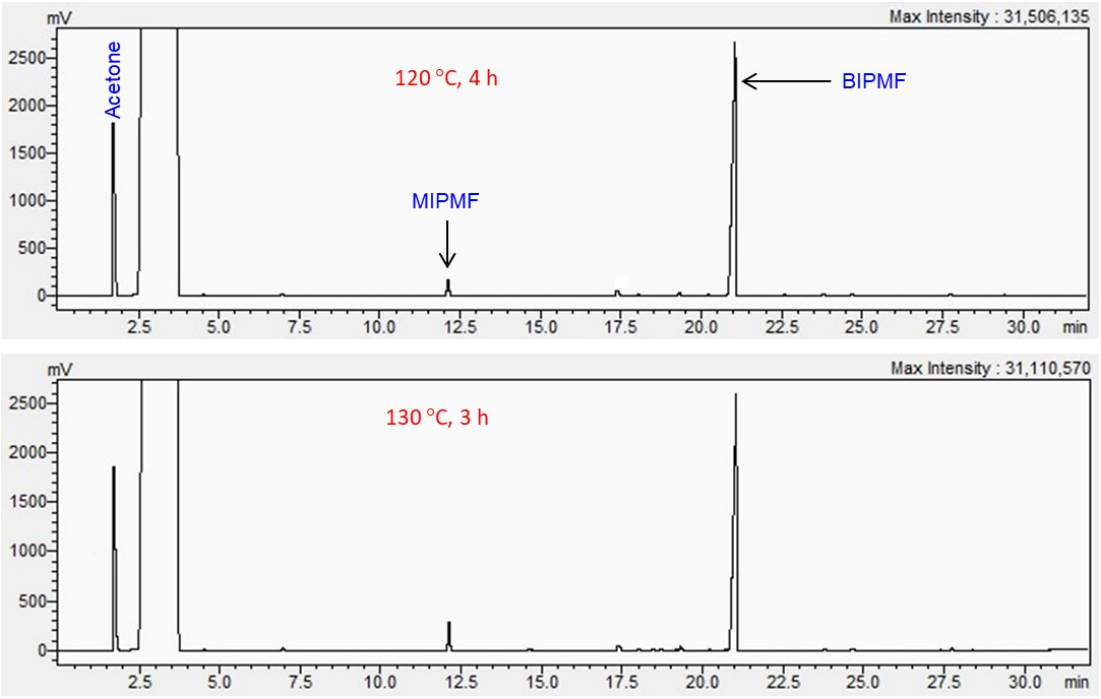

Fig. S13 GC chromatograms for the one-pot reductive etherification of HMF to BIPMF over Zr-BDC-S_{60}. Reaction conditions: 0.25 g HMF, 19.75 g iPrOH, 0.1 g catalyst.

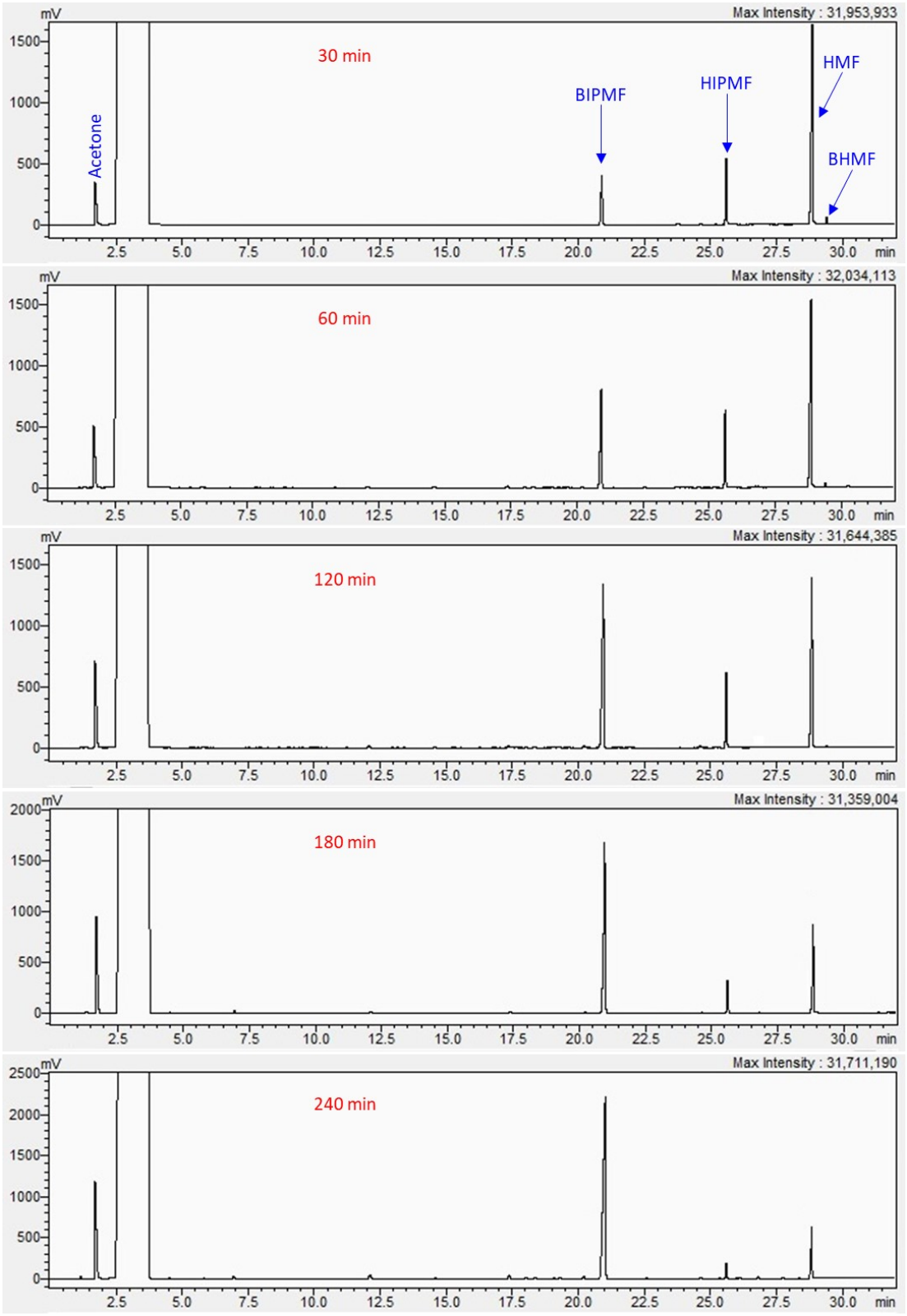

Fig. S14 GC chromatograms for the one-pot reductive etherification of HMF to BIPMF over Zr-BDC-S_{60} at 90 °C. Reaction conditions: 0.25 g HMF, 19.75 g iPrOH, 0.1 g catalyst.

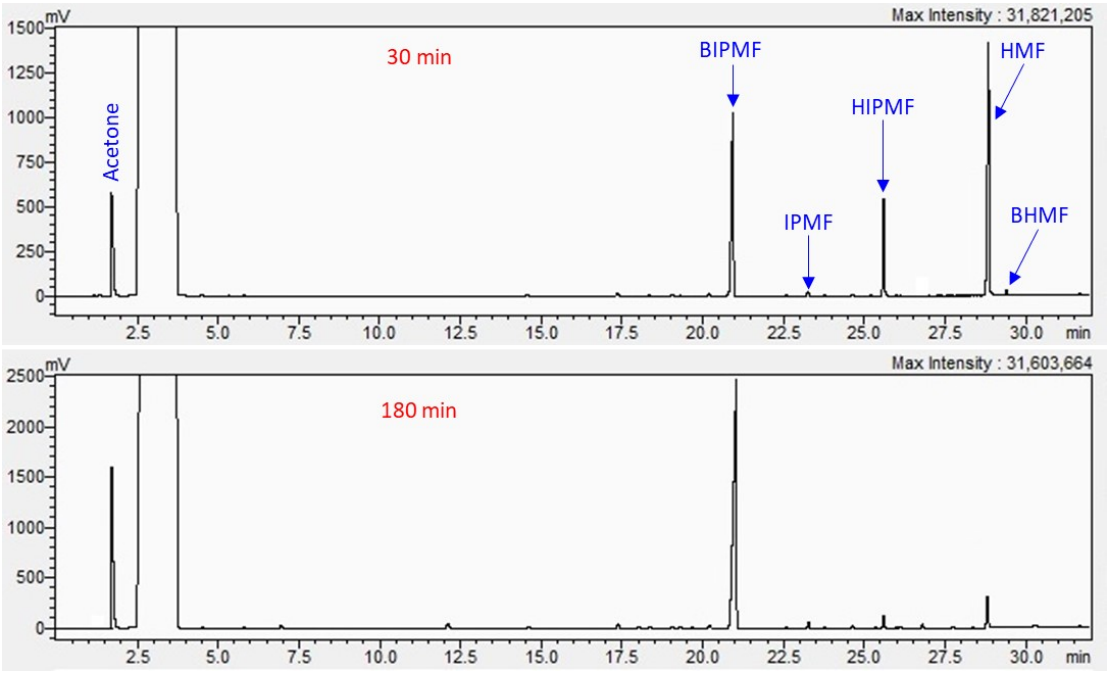

Fig. S15 GC chromatograms for the one-pot reductive etherification of HMF to BIPMF over Zr-BDC-S_{60} at 100 °C. Reaction conditions: 0.25 g HMF, 19.75 g iPrOH, 0.1 g catalyst.

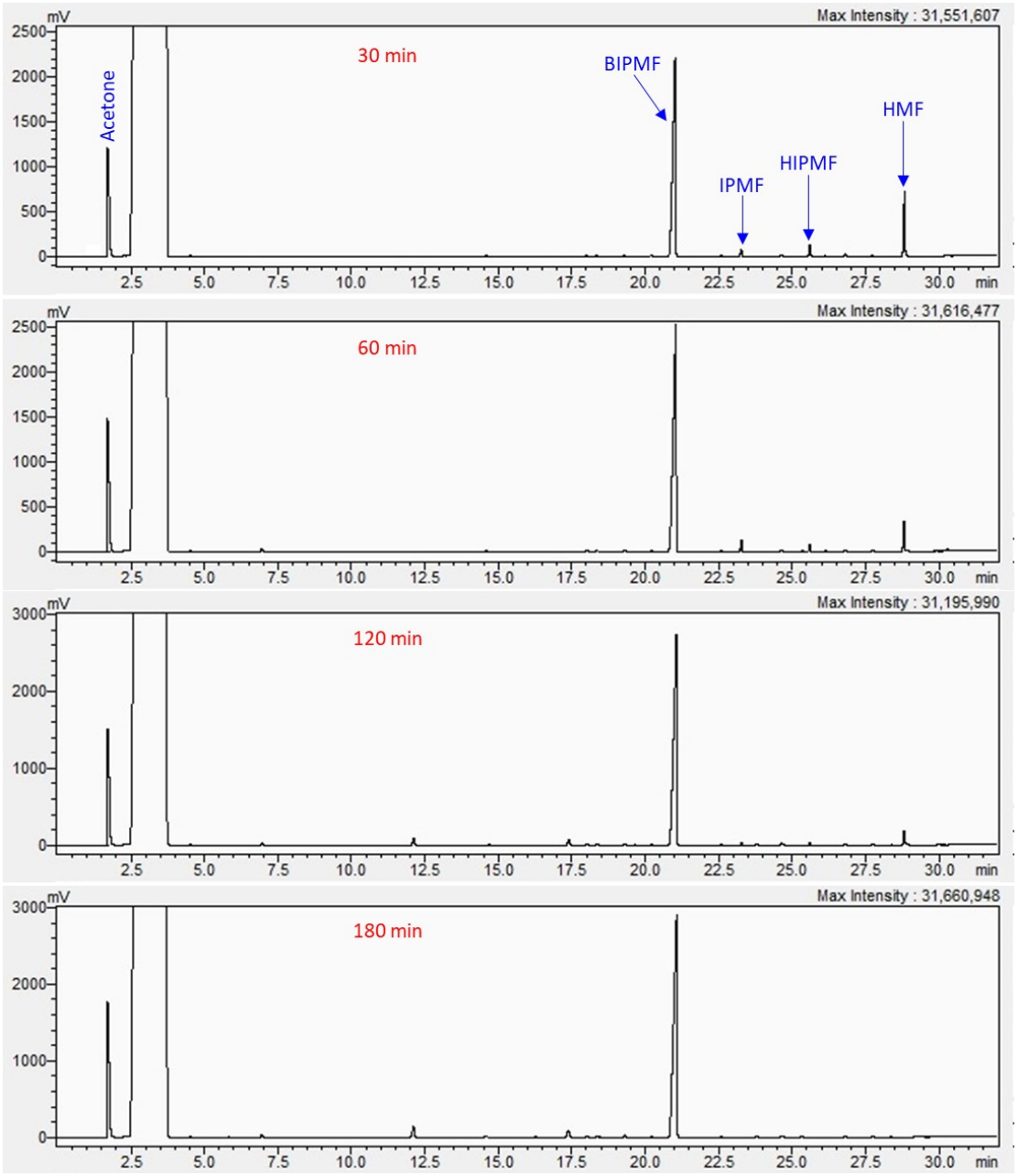

Fig. S16 GC chromatograms for the one-pot reductive etherification of HMF to BIPMF over Zr-BDC-S_{60} at 120 °C. Reaction conditions: 0.25 g HMF, 19.75 g iPrOH, 0.1 g catalyst.

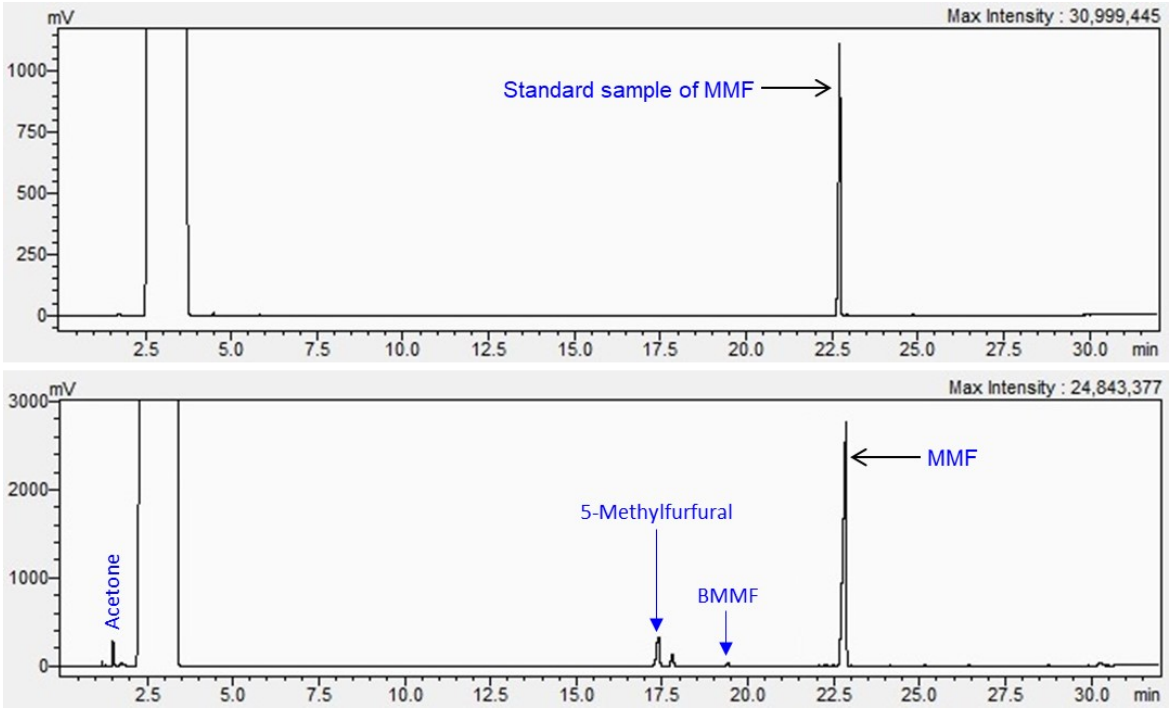

Fig. S17 GC chromatograms for the one-pot reductive etherification of HMF in MeOH over Zr-BDC-S_{60}. Reaction conditions: 0.25 g HMF, 19.75 g MeOH, 0.1 g catalyst, 120 °C, 3 h.

Table S1 Physicochemical properties of various catalysts

Catalyst	Surface area (m^2/g)[a]	Pore volume (cm^3/g)[b]	Pore size (nm)[b]	Acid content (mmol/g)[c]	Base content (mmol/g)[d]	L/B ratio[e]
ZrO_2	26.5	0.062	9.2	0.08	0.11	—
$ZrCl_4$	—	—	—	—	—	—
BDC	—	—	—		—	—
BDC-SO_3H	—	—	—		—	—
Zr-BDC	589.4	0.443	2.6	0.745	1.182	19.51/20.03
Zr-BDC-S_{60}	321.9	0.278	3.5	1.289	1.834	2.32/2.41
Zr-BDC-S_{100}	53.8	0.107	9.4	1.426	1.963	1.29/1.35
Sn-BDC-S_{60}	158.5	0.186	4.2	0.881	1.237	1.98/2.12
Zr-BDC-S_{60}[f]	280.7	0.252	3.3	1.154	1.685	—

[a] Surface areas were obtained by the method of BET. [b] Pore volumes and pore sizes were estimated by the method of BJH. [c] Acid contents were determined by the profiles of NH_3-TPD. [d] Base contents were determined by the profiles of CO_2-TPD. [e] L/B ratios were measured by the profiles of pyridine-adsorbed FT-IR at 110 °C and 250 °C. [f] The catalyst was reused five reaction runs.

Table S2 EA and ICP-AES of the fresh and spent Zr-BDC-S_{60}

Catalyst	Element content (%)			
	C[a]	S[a]	H[a]	Zr[b]
Fresh	29.68	2.61	1.94	24.43
Spent	33.81	2.44	2.03	23.91

[a] C, S and H were measured by EA. [b] Zr was measured by ICP-AES.

Reference

1 J. Wei, T. Wang, H. Liu, M. Z. Li, X. Tang, Y. Sun, X. Zeng, L. Hu, T. Lei and L. Lin, *Energy Technol.*, 2019, **7**, 1801071.

2 W. Wang, H. Wang, X. Jiang, Z. He, Y. Yang, K. Wang and Z. Liu, *ACS Sustain. Chem. Eng.*, 2022, **10**, 4969-4979.